The copolymer blending method

Wright, Daniel B.; Patterson, Joseph P.; Pitto-Barry, Anais; Lu, Annhelen; Kirby, Nigel; Gianneschi, Nathan C.; Chassenieux, Christophe; Colombani, Olivier; O'Reilly, Rachel K.

[Link to publication on Research at Birmingham portal](#)

Download date: 20. Apr. 2024

Macromolecules

Article

The Copolymer Blending Method: A New Approach for Targeted Assembly of Micellar Nanoparticles

Daniel B. Wright,[†] Joseph P. Patterson,[§] Anaïs Pitto-Barry,[†] Annhelen Lu,[†] Nigel Kirby,[‖] Nathan C. Gianneschi,[§] Christophe Chassenieux,*[‡] Olivier Colombani,*[‡] and Rachel K. O'Reilly*[†]

[†]Department of Chemistry, University of Warwick, Gibbet Hill Road, Coventry CV4 7AL, U.K.

[‡]Département PCI, Université du Maine, Avenue Olivier Messiaen, 72085 Le Mans, Cedex 09, France

[§]Department of Chemistry & Biochemistry, University of California, San Diego, 9500 Gilman Drive, La Jolla, California 92093, United States

[‖]Australian Synchrotron, 800 Blackburn Road, Clayton, Victoria 3168, Australia

S Supporting Information

ABSTRACT: Polymer self-assembly in solution is a simple strategy for the preparation of elegant yet complex nanomaterials. However, exhaustive synthesis of the copolymer synthons is often required to access specific assemblies. In this work we show that the blending of just two diblock copolymers with identical block lengths but varying hydrophobic monomer incorporations can be used to access a range of assemblies of intermediate hydrophobic composition. Indeed, the nanostructures produced from blending are identical to those formed with the directly synthesized copolymer of the same composition. This new approach presents researchers with a more efficient and accessible methodology to access precision self-assembled nanostructures, and we highlight its potential by applying it to a demonstrator catalytically active system.
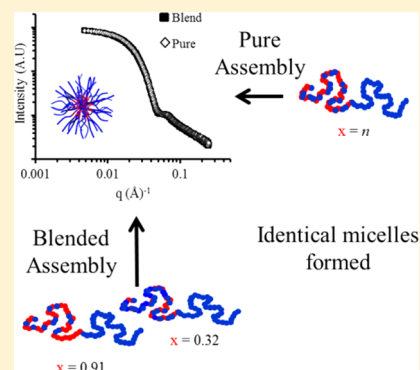
Nature captivates us with its ability to produce precise supramolecular nanostructures in highly competitive environments. In soft nanotechnology, attempts have been made to mimic the form and function of Nature's nanostructures using amphiphilic block copolymers which spontaneously self-assemble in selective solvents.[1−3] These synthetic nanostructures have enormous potential in a variety of applications including delivery agents, imaging, and enhanced oil recovery.[4−9] However, for an amphiphilic block copolymer to be specific to a desired application, the chemical structure must be adapted to yield the desired characteristics on the nanoscale in terms of size, aggregation number, functionality, and often response to an external stimulus.[10−12] This explains partly why a plethora of amphiphilic block copolymers and associated assembled nanostructures can be found in the literature, each new nanostructure requiring a new polymer and therefore a new synthetic batch.

To overcome this problem of laborious custom polymer synthesis for every desired nanostructure, an attractive strategy would be to blend two polymers, differing in terms of structural characteristics and stimuli response, to obtain a range of blends exhibiting characteristics between those of the two polymers.[13−21] This strategy would provide a route for accessing a wide range of functional properties or responses to stimuli, with only two polymers blended at various stoichiometry rather than a different polymer for each desired property.

Although previous reports exist on the blending of diblock copolymers, these reports have utilized blending to explore polymer morphologies that are typically not accessed through the self-assembly of a single polymer system.[22−24] In contrast here, our strategy was to blend two block−random diblock copolymers for a targeted assembly approach where specific polymer assemblies with precise characteristics could then be generated. Here the block−random diblock copolymers consist of a homopolymeric hydrophilic block connected to a hydrophobic block containing both hydrophilic and hydrophobic units statistically distributed.[25] The use of such polymers presents two assets. First, it has been shown recently that modifying the ratio of hydrophilic to hydrophobic units distributed statistically in the associating block allowed for tunable characteristics of the assemblies in water in terms of aggregation and resulting properties.[26−33] Moreover, incorporating hydrophilic units within the hydrophobic block of such polymers moderates their hydrophobicity so that the resulting self-assembled structures are in dynamic equilibrium with free unassembled chains (unimers).[27−30,33] It must be realized that this second aspect is a prerequisite of the utmost importance for the proposed targeted assembly strategy. Indeed, most amphiphilic block copolymers described in the literature lead to
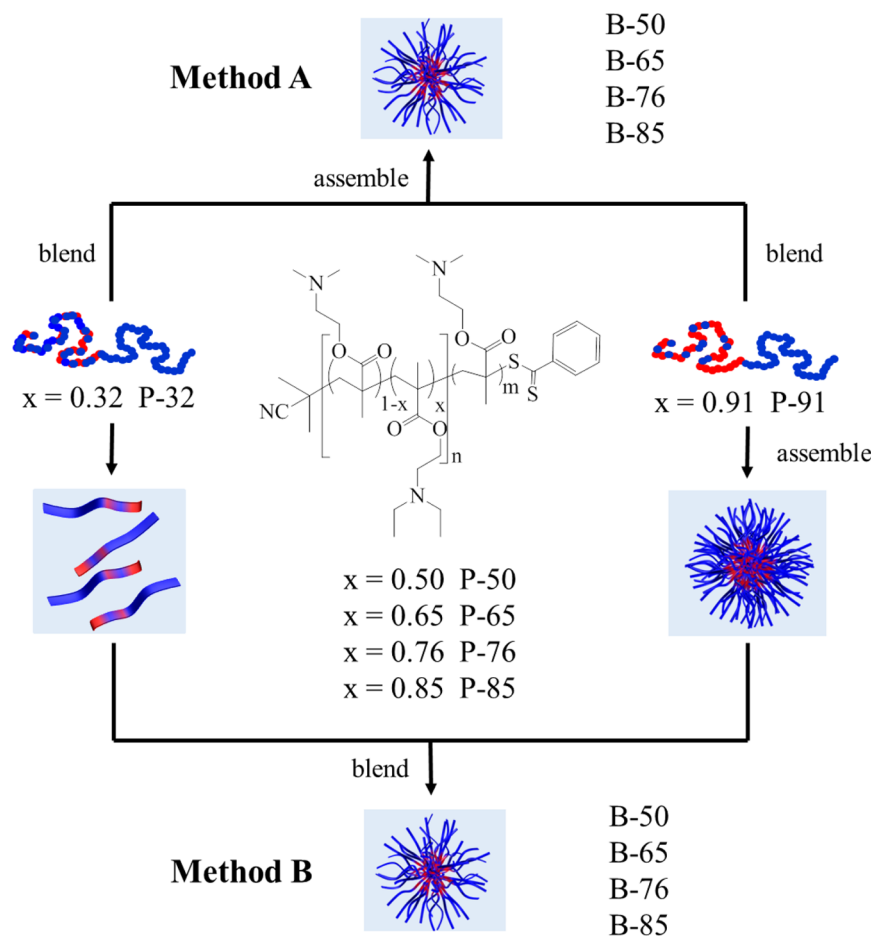
Figure 1. Schematic demonstrating the blending protocols employed. Center: schematic of the P(DMAEMA-co-DEAEMA)-b-PDMAEMA diblock copolymers. Method A: dry powder mixing (unimer blending); polymers are first mixed in the unimer state to match the desired DEAMEA n % and then subsequently assembled. Method B: micelle blending; polymers are first solubilized separately and then mixed to match the desired DEAEMA n %. Using method B, **P-91** is already assembled whereas **P-32** exists as unimers at $\alpha = 0$.

"frozen" self-assemblies.[34] Since these out-of-equilibrium structures are unable to reorganize, two micelles consisting of different polymers could not rearrange into mixed micelles. Indeed, even if the mixing was thermodynamically possible, it would be prevented for kinetic reasons.[16,18,20,24,34−38]

Our strategy consisted in mixing two block−random copolymers differing only in the ratio of comonomers in order to form blended micelles whose size and aggregation number depended on the content of each block−random copolymer in the blend. This simple blending protocol allows us to tune the characteristics of blended micelles in solution by simple formulation rather than by a demanding synthetic approach. Moreover, the blended micelles were structurally identical to those formed by a single block−random copolymer matching the overall composition of the blend. Given the simplicity of this method, we extended it to a catalytically active L-proline system, allowing us to specifically target precise and isolated catalytic pockets mimicking those found in natural biological systems.

RESULTS AND DISCUSSION

Formation of Blended Micelles. First, we studied the self-assembly in aqueous solution of blends of two P(DMAEMA-co-DEAEMA)-b-PDMAEMA diblock copolymers (DMAEMA: N,N-dimethylaminoethylmethacrylate, DEAEMA: N,N-diethylaminoethylmethacrylate) (Figure 1) containing respectively 32

mol% (**P-32**, where P stands for "pure") and 91 mol% (**P-91**) of DEAEMA in the core-forming block. Altering the ratio of these two polymers in the blend allowed us to target different DEAEMA contents (**B-50**, **B-65**, **B-76**, and **B-85**, where B stands for "blend"). The behavior of the blends could then be compared with that of pure P(DMAEMA-co-DEAEMA)-b-PDMAEMA polymers with the same average composition (**P-50**, **P-65**, **P-76**, and **P-85**), but where all chains are quasi-identical. The synthesis and characterization in aqueous solution of the pure diblock copolymers with varying DEAEMA incorporation were reported previously (Table 1).[33]

Here, all polymers were studied at $\alpha = 0$ in 0.1 M NaCl solution, and thus all DEAEMA units are hydrophobic. α represents the overall ionization degree of the DEAEMA and DMAEMA units; that is, the ratio of these units that are positively charged. Note that at $\alpha = 0$ **P-91** self-assembles into spherical micelles, whereas **P-32** remains as unimers. Two methods of preparation were used to verify if equilibrium was reached and that blended micelles were obtained by the coassembly of **P-91** and of **P-32** rather than a mixture of micelles of **P-91** and unimers of **P-32**. Method A (unimer blending, Figure 1) consisted of mixing bulk polymer powders and dissolving the polymers at $\alpha = 1$ and finally lowering the value of α to 0. With this method, the starting solution is a mixture of unimers, which probably favors the formation of blended micelles as thermodynamic equilibrium is reached

Table 1. Characteristics of the P(DMAEMA$_{1-x}$-co-DEAEMA$_x$)$_n$-b-PDMAEMA$_m$ Diblock Copolymers

diblock copolymer	x^a	n^b	m^b	$M_{n,NMR}^b$ (kDa)	$M_{n,SEC}^c$ (kDa)	$Đ_{SEC}^c$
P-32	0.32	35	30	10.7	13.8	1.16
P-50	0.50	34	32	11.1	13.4	1.18
P-65	0.65	36	35	12.3	14.2	1.12
P-76	0.76	25	34	10.0	12.8	1.18
P-85	0.85	31	35	11.4	13.9	1.17
P-91	0.91	28	32	10.4	13.5	1.10

^{a}Determined by ^{1}H NMR spectroscopy using the signals at δ = 4.20 and 2.10 ppm. ^{b}Determined by end-group analysis from ^{1}H NMR spectroscopy. ^{c}From SEC based on poly(methyl methacrylate) standards and DMF as the eluent.

upon decrease of α, the solvent quality for the core-forming block.[39,40] For method B, (micelle blending, Figure 1), P-32 and P-91 are first dispersed independently and then blended only once they have reached α = 0. If unimer exchange does not occur, no blended micelles are expected to form due to kinetic limitations.

First, it can be seen in Figures 2a and 2b that steady state is only reached after several days with method B, the micelle blending route, whereas with method A blended micelles are formed after 1 day. However, both methods lead to the same structures being formed (Figure 2c), which is strongly

indicative of both blend systems being at equilibrium. At equilibrium (final blend state), the weight-average aggregation number of the micelles is strongly different from the value expected for a mixture of nonblended P-91 micelles and P-32 unimers (shown as the straight line in Figure 2a) which can be calculated according to eq 1, where C is the weight concentration of the polymers in solution. It can be concluded that no matter the preparation method, P-32 and P-91 co-assemble at α = 0 into blended micelles where the structure is governed by the blending ratio of the two parent polymers.

$$N_{agg,mix} = \frac{C_{P-91}N_{agg,P-91} + C_{P-32}N_{agg,P-32}}{C_{P-91} + C_{P-32}} \quad (1)$$

Since blended micelles are formed even with method B and taking into account that these hybrid micelles are smaller in aggregation number than the initial P-91 micelles, it can be deduced that unimer exchange does occur, causing the formation of the blended micelles.[41−43] It should be noted that for star-like micelles R_h only weakly depends on N_{agg}; hence, N_{agg} varied during the reorganization but R_h was hardly affected.[44] Additional small-angle X-ray scattering (SAXS) studies (Figures 2b,d) confirm this exchange of unimers to form blended micelles. From the Porod representation (Figure 2b), the shift in the first oscillation is clearly visible, highlighting the reorganization to blended micelles over time. Furthermore, when the first minima in the SAXS profiles (Figure 2d) are
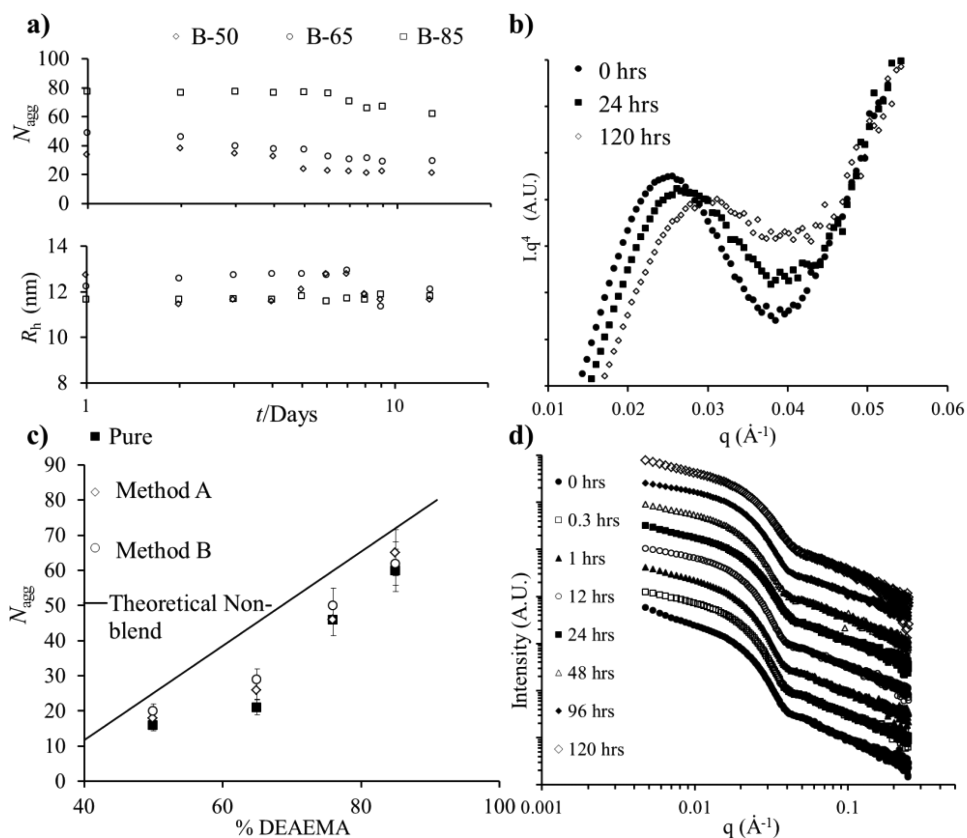

Figure 2. (a) Evolution of aggregation number (N_{agg}) and hydrodynamic radius R_h with time upon blending stock solutions using method B. (b) Porod representation of the SAXS data for **B-76** with time at 2.5 g/L. (c) Relationship of the aggregation number (N_{agg}) at steady state for both blending methods A and B and theoretical aggregation number for a nonblended mixture (straight line) from eq 1 with % DEAEMA in the core domain. N_{agg} of the pure micelles of the same composition as the blends are also given. Error bars are calculated from 10% of the N_{agg} values. (d) SAXS profiles of **B-76** at 2.5 g/L over time; 0 hours indicates the start of the blending for method B. Plots have been shifted vertically for clarity; see Supporting Information for SAXS fits.

compared, we observe a shift to larger q values (from 0.042 to 0.046 Å^{-1}). Both the shifts in Figures 2b,d are representative of a reduction in the core size of the micelles. This reduction in core size is attributed to a decrease in aggregation number as the formation of blended micelles occurs, which is consistent with the light scattering results (Figure 2a).[45]

Structural Comparison of Blended Micelles and Pure Micelles. The blended micelles formed by mixing different ratios of **P-32** and **P-91** (using method A, unimer blending) were compared to those obtained with a pure diblock copolymer matching the average chemical composition of the blend. For these samples, laser light scattering (LLS) (Figures 2c and 3a), SAXS (Figure 3b), and cryogenic transmission
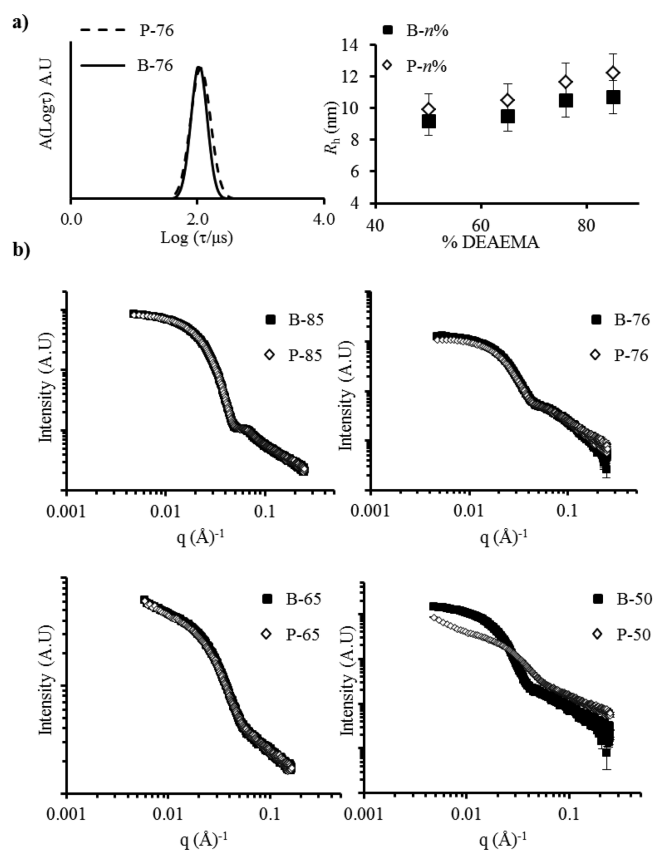

Figure 3. (a) Left pane: relaxation time distribution from DLS of **P-76** and **B-76** at $\alpha = 0$ in 0.1 M NaCl, at 2.5 g/L obtained by dynamic light scattering; right pane: dependence of hydrodynamic radius (R_h) with % DEAEMA in the core domain. Error bars are calculated from 10% of the R_h values. (b) SAXS profiles of blended and pure samples in NaCl 0.1 M at 2.5 g/L. Note that for the 85%, 76%, and 65% samples the profiles superimpose for the blended and pure solutions. See Table 2 and Table S4 for SAXS fits. All samples were prepared using assembly method A.

electron microscopy (cryo-TEM) (Figure 4) were used to analyze the size (R_h and R_c) of the blended and pure micelles. Remarkably for both the blended and pure micelles above 50% DEAEMA the core sizes are structurally indistinguishable to one another when any of the analysis methods are used (Figure 4 and see Supporting Information for micelle dimensions from SAXS data fits and additional cryo-TEM analysis). However, it should be noted that for 50% DEAEMA (Figure 3b, bottom right pane), a difference between the blended and pure samples is observed. At this composition the pure micelles are only
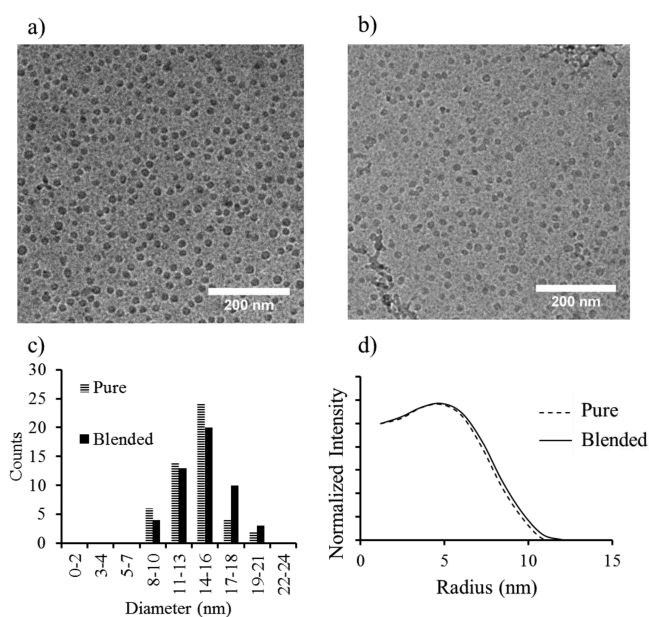

Figure 4. Cryo-TEM analysis of both **P-85** and **B-85** prepared by method A: (a) image of **P-85**; (b) image of **B-85**. (c) Histograms of the core diameter for both **P-85** and **B-85** samples. (d) Radial plot profiles from cryo-TEM for both **P-85** and **B-85** samples (averaged over 50 particles).

weakly associated and exhibit very little contrast between the core and corona. This correlates with critical aggregation concentration studies, CAC (see Supporting Information), where the association of **P-91** was proposed to drive the association of the blended micelles. Furthermore, the blended samples contain a highly aggregating species, and it is hypothesized that this species gives an increased core−corona contrast for the blend assembly. Nevertheless, as both blended and pure systems observed are identical, it is believed that the systems reach equilibrium, where a system at dynamic equilibrium allows for successful blending.[24,46]

Both SAXS and cryo-TEM have the benefit of being able to directly probe the core size of the micellar aggregates in addition to LLS, which allows a theoretical core size to be calculated using eq S6. This allows a comparison of three techniques (LLS, cryo-TEM, and SAXS) to fully analyze the blended and pure micelles (Table 2). A general trend observed is that a decrease in DEAEMA content (from 85% to 50%) gave smaller core sizes. However, the core sizes from cryo-TEM

Table 2. Additional Micelle Scattering Characterization Data for All Blended and Pure Samples at $\alpha = 0$ in 0.1 M NaCl Solution

	$R_{c,LLS}$ (nm)[a]	$R_{c,cryo-TEM}$ (nm)	$R_{c,SAXS}$ (nm)	core density based on cryo-TEM[b] (g/L)
P-85	5.1	7.8	8.6	0.17
P-76	4.6	7.8	8.7	0.12
P-65	3.9	6.5	7.6	0.09
P-50	3.3	7.0	5.0	0.05
B-85	5.3	7.3	8.6	0.20
B-76	4.8	7.7	8.8	0.14
B-65	3.9	6.8	7.5	0.09
B-50	3.5	7.4	9.9	0.06

[a]Calculated from eqs S6 and S9 assuming a core density of 1 g/L. [b]Calculated from eq S6 using R_c from cryo-TEM and N_{agg} from SLS.
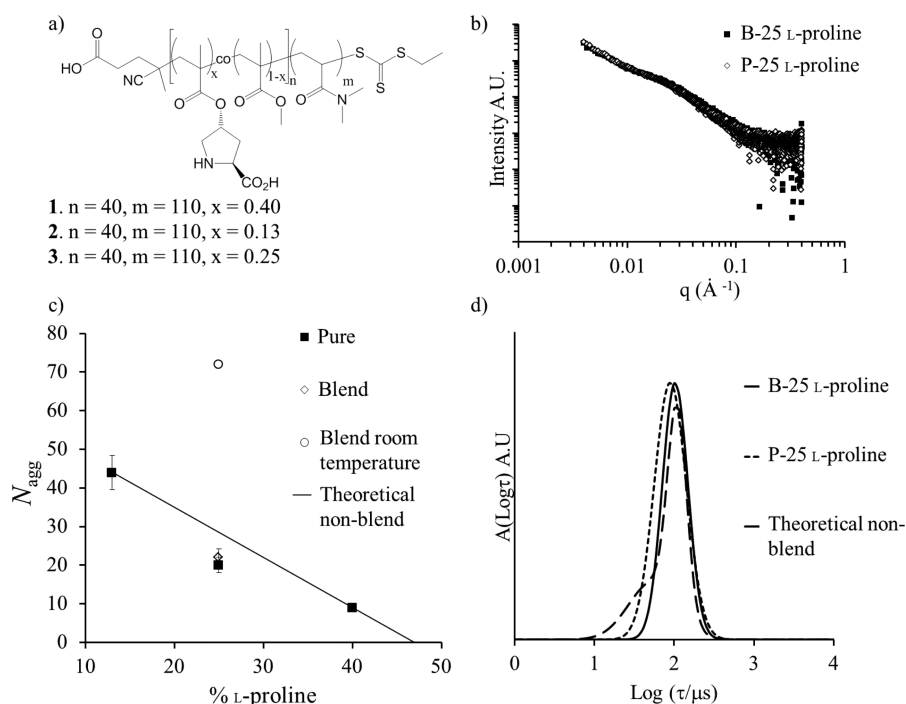
Figure 5. Data for the blended L-proline micelles prepared using unimer blending, method A. (a) Structure of the L-proline diblock copolymers. (b) SAXS analysis of pure and blended L-proline diblock copolymers, at 2.5 g/L note that the profiles superimpose for the blended and pure solutions (see Supporting Information for SAXS fits). (c) Relationship of the experimental aggregation number (N_{agg}) of the blends and of the pure micelles with the same composition with changing % L-proline in the core domain. N_{agg} of the pure micelles of the same composition as the blends are also given. Error bars are calculated from 10% of the N_{agg} values. (d) Relaxation distribution of the pure micelles and blended micelles (at 2.5 g/L) and a theoretical distribution for a nonblended mixture.

and SAXS give slightly larger sizes than calculated from the N_{agg} determined by LLS, which can be attributed to the small contrast difference between the core and corona; therefore, the corona is partially seen.

The core size determined from LLS is calculated assuming that the density of the core is equal to that of the bulk density of the two monomers and is assumed to be constant. However, by using a combination of LLS and cryo-TEM, the core density can be explored further; specifically, a decrease in core density is attributed to an increase in the hydration of the core. This core analysis was explored using a combination of Z-average core sizes from cryo-TEM and N_{agg} values from LLS to predict the core density using eq S6; however, the calculated core densities, approximately <0.2 g/mL (Table 2), are too low to provide significant contrast for cryo-TEM, which leads us to believe that the corona must be visible. Moreover, the difference in the scattering length densities between the two monomers for SAXS analysis is extremely small (4.8×10^{-8} Å^{-2}), which results in a portion of the coronal chains being included in the core size when analyzed by SAXS.

Application to Catalytically Active Micelles. This blending method provides a simple and effective route to achieve defined nanoscale assemblies without laborious synthetic approaches. These results demonstrate that the blending strategy can be used to screen both the morphology and function of pure diblock copolymer micelles which can then be adapted for a target application. To highlight the utility of this new approach, we investigated the blending of three diblock copolymers (Figure 5a), with varying incorporations of L-proline in the core domain, to form catalytically active nanostructures.

This strategy allows us to compare the catalytic activity of the pure and blended micelle assemblies and confirm that the proposed strategy is not only relevant from a fundamental point of view but can be used to prepare functional assemblies with targeted properties. As these L-proline block copolymers chemically differ from the pH-responsive methacrylate polymers shown previously, the assembly procedure for these particles was slightly modified (see Supporting Information for details).

Briefly, the powders were mixed and dispersed in water. However, due to the high T_g of methyl methacrylate in the core block, dynamic equilibrium was not reached at room temperature. The solutions were therefore heated to 75 °C for 4 h. The increase in temperature allows for the core block to become more mobile and reduces the energy barrier for molecular exchange thus allowing equilibrium to be reached,[34] resulting in a reorganization of the system as revealed by the difference between the heated and non-heated solutions in Figure 5c.

This reorganization was the first suggestion that blending did occur, provided that the mixing was done at sufficiently high temperature. This was further confirmed using eq S10 which allows for a theoretical relaxation times distribution to be calculated for a nonblended mixture of micelles (see Supporting Information for details). As shown in Figure 5d, the theoretical relaxation distribution does not match the experimentally observed value, indicating that blended micelles are formed rather than a simple mixture of two micelles of different compositions.

Moreover, for these three polymers it was observed that the blended micelles which are formed are identical to the pure copolymer assemblies (Figures 5b,c).
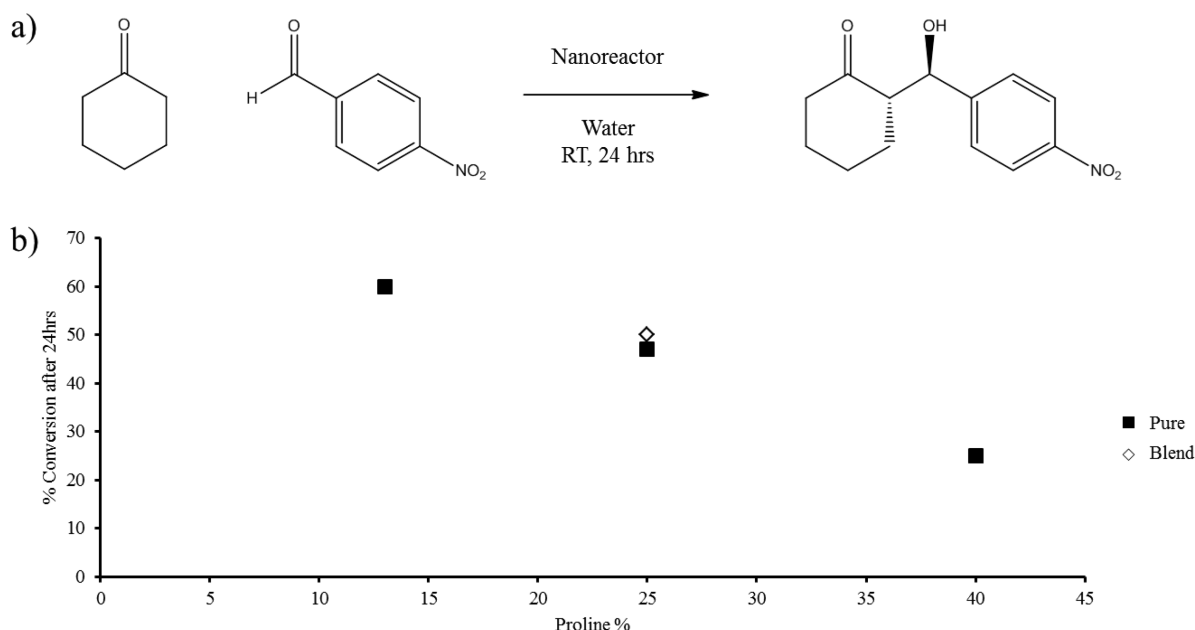
Figure 6. (a) Aldol reaction of 4-nitrobenzaldehyde and cyclohexanone catalyzed by L-proline micelles. (b) Aldol catalysis data for 1 mol% catalyst loading for the pure and blended micelles as determined by ¹H NMR spectroscopy.

To understand and evaluate the catalytic performance of these blended micelles compared to the pure micelles, an aldol reaction was undertaken (Figure 6a). An increase in the L-proline content in the core gives a decrease in the conversion after 24 h as previously reported (Figure 6b).[47] The kinetics of the aldol catalysis using the blended (47% conversion for B-25) and pure micelles (50% conversion for P-25) were very similar (Figure 6b).

Given that the concentration of catalyst was constant in these reactions and previous work suggests that the structure of these L-proline micelles dictates the catalytic activity,[48] we can infer that the catalytic environment created in both assemblies are identical. This emphasizes that the copolymer blending method, in which two copolymers of differing compositions are blended, produces micelles which have not only the same structure but the same function as the assemblies prepared from the assembly of a precision copolymer of the same composition.

CONCLUSIONS

A simple copolymer blending method has been utilized to produce a range of polymeric micelles in aqueous solution. In this approach two copolymers with high and low incorporations of hydrophobic monomer are blended to afford a variety of polymeric micelles with varying intermediate hydrophobic compositions. By a combination of cryo-TEM, laser light, and small-angle X-ray scattering methods, these blended micelles were found to be structurally identical to pure micelles with the same composition formed from the direct assembly of a single compositionally pure polymer diblock. This work represents an advantage over traditional approaches for the preparation of spherical nanostructures with specific structural characteristics as it requires minimal synthesis and allows access to the full range of intermediate copolymer compositions through a simple blending approach rather than exhaustive synthesis. We propose this new methodology as a simple, scalable, and effective route to obtain functional block copolymer micelles of diverse compositions and properties as desired for applications such as drug delivery vehicles, stabilizers, or catalytic reactors.

ASSOCIATED CONTENT

Ⓢ Supporting Information

The Supporting Information is available free of charge on the ACS Publications website at DOI: 10.1021/acs.macromol.5b01426.

> Additional characterization data, SLS and DLS data, SAXS data, cryo-TEM images, and CAC fluorescent experiments for polymers **P-32−P-91**, **B-50−B-85**, and L-proline polymers (PDF)

AUTHOR INFORMATION

Corresponding Authors

*E-mail: R.K.O-Reilly@warwick.ac.uk (R.K.O.).

*E-mail: olivier.colombani@univ-lemans.fr (O.C.).

*E-mail: christophe.chassenieux@univ-lemans.fr (C.C.).

Notes

The authors declare no competing financial interest.

ACKNOWLEDGMENTS

REFERENCES

(1) Hamley, I. W. *The Physics of Block Copolymers*; Oxford University Press: Oxford, 1998.

(2) Hamley, I. W. *Block Copolymers in Solution: Fundamentals and Applications*; Wiley: New York, 2005.

(3) Hayward, R. C.; Pochan, D. J. *Macromolecules* **2010**, *43*, 3577.

(4) Chien, M.-P.; Carlini, A. S.; Hu, D.; Barback, C. V.; Rush, A. M.; Hall, D. J.; Orr, G.; Gianneschi, N. C. *J. Am. Chem. Soc.* **2013**, *135*, 18710.

(5) Bai, Z.; Lodge, T. P. *J. Am. Chem. Soc.* **2010**, *132*, 16265.

(6) Lodge, T. P.; Rasdal, A.; Li, Z.; Hillmyer, M. A. *J. Am. Chem. Soc.* **2005**, *127*, 17608.

(7) Rees, P.; Wills, J. W.; Brown, M. R.; Tonkin, J.; Holton, M. D.; Hondow, N.; Brown, A. P.; Brydson, R.; Millar, V.; Carpenter, A. E.; Summers, H. D. *Nat. Methods* **2014**, *11*, 1177.

(8) Hudson, Z. M.; Lunn, D. J.; Winnik, M. A.; Manners, I. *Nat. Commun.* **2014**, *5*, 3372.

(9) Wever, D. A. Z.; Picchioni, F.; Broekhuis, A. A. *Prog. Polym. Sci.* **2011**, *36*, 1558.

(10) Lu, A.; O'Reilly, R. K. *Curr. Opin. Biotechnol.* **2013**, *24*, 639.

(11) Kelley, E. G.; Albert, J. N. L.; Sullivan, M. O.; Epps, T. H., III *Chem. Soc. Rev.* **2013**, *42*, 7057.

(12) Cotanda, P.; Wright, D. B.; Tyler, M.; O'Reilly, R. K. *J. Polym. Sci., Part A: Polym. Chem.* **2013**, *51*, 3333.

(13) Renou, F.; Nicolai, T.; Nicol, E.; Benyahia, L. *Langmuir* **2009**, *25*, 515.

(14) Palyulin, V. V.; Potemkin, I. I. *Macromolecules* **2008**, *41*, 4459.

(15) Sens, P.; Marques, C. M.; Joanny, J. F. *Macromolecules* **1996**, *29*, 4880.

(16) Tian, M. M.; Qin, A. W.; Ramireddy, C.; Webber, S. E.; Munk, P.; Tuzar, Z.; Prochazka, K. *Langmuir* **1993**, *9*, 1741.

(17) Cantu, L.; Corti, M.; Salina, P. *J. Phys. Chem.* **1991**, *95*, 5981.

(18) Calderara, F.; Riess, G. *Macromol. Chem. Phys.* **1996**, *197*, 2115.

(19) Borovinskii, A. L.; Khokhlov, A. R. *Macromolecules* **1998**, *31*, 7636.

(20) Yoo, S. I.; Sohn, B.-H.; Zin, W.-C.; Jung, J. C.; Park, C. *Macromolecules* **2007**, *40*, 8323.

(21) Hillmyer, M. A. *J. Polym. Sci., Part B: Polym. Phys.* **2007**, *45*, 3249.

(22) Yan, N.; Yang, X.; Zhu, Y.; Xu, J.; Sheng, Y. *Macromol. Chem. Phys.* **2012**, *213*, 2261.

(23) Schuetz, P.; Greenall, M. J.; Bent, J.; Furzeland, S.; Atkins, D.; Butler, M. F.; McLeish, T. C. B.; Buzza, D. M. A. *Soft Matter* **2011**, *7*, 749.

(24) Jain, S.; Bates, F. S. *Macromolecules* **2004**, *37*, 1511.

(25) Tsitsilianis, C.; Gotzamanis, G.; Iatridi, Z. *Eur. Polym. J.* **2011**, *47*, 497.

(26) Shedge, A.; Colombani, O.; Nicolai, T.; Chassenieux, C. *Macromolecules* **2014**, *47*, 2439.

(27) Charbonneau, C. l.; Chassenieux, C.; Colombani, O.; Nicolai, T. *Macromolecules* **2011**, *44*, 4487.

(28) Lejeune, E.; Drechsler, M.; Jestin, J.; Muller, A. H. E.; Chassenieux, C.; Colombani, O. *Macromolecules* **2010**, *43*, 2667.

(29) Bendejacq, D. D.; Ponsinet, V. *J. Phys. Chem. B* **2008**, *112*, 7996.

(30) Bendejacq, D. D.; Ponsinet, V.; Joanicot, M. *Langmuir* **2005**, *21*, 1712.

(31) Borisova, O.; Billon, L.; Zaremski, M.; Grassl, B.; Bakaeva, Z.; Lapp, A.; Stepanek, P.; Borisov, O. *Soft Matter* **2011**, *7*, 10824.

(32) Ribaut, T.; Oberdisse, J.; Annighofer, B.; Stoychev, I.; Fournel, B.; Sarrade, S.; Lacroix-Desmazes, P. *Soft Matter* **2009**, *5*, 4962.

(33) Wright, D. B.; Patterson, J. P.; Pitto-Barry, A.; Cotanda, P.; Chassenieux, C.; Colombani, O.; O'Reilly, R. K. *Polym. Chem.* **2015**, *6*, 2761.

(34) Nicolai, T.; Colombani, O.; Chassenieux, C. *Soft Matter* **2010**, *6*, 3111.

(35) Lund, R.; Willner, L.; Richter, D.; Dormidontova, E. E. *Macromolecules* **2006**, *39*, 4566.

(36) Stejskal, J.; Hlavatá, D.; Sikora, A.; Konňák, Č.; Pleštil, J.; Kratochvíl, P. *Polymer* **1992**, *33*, 3675.

(37) Choi, S.-H.; Lodge, T. P.; Bates, F. S. *Phys. Rev. Lett.* **2010**, *104*, 047802.

(38) Won, Y. Y.; Davis, H. T.; Bates, F. S. *Macromolecules* **2003**, *36*, 953.

(39) Mai, Y.; Eisenberg, A. *Chem. Soc. Rev.* **2012**, *41*, 5969.

(40) Meli, L.; Santiago, J. M.; Lodge, T. P. *Macromolecules* **2010**, *43*, 2018.

(41) Nose, T.; Iyama, K. *Comput. Theor. Polym. Sci.* **2000**, *10*, 249.

(42) Halperin, A.; Alexander, S. *Macromolecules* **1989**, *22*, 2403.

(43) Nyrkova, I. A.; Semenov, A. N. *Macromol. Theory Simul.* **2005**, *14*, 569.

(44) Daoud, M.; Cotton, J. P. *J. Phys. (Paris)* **1982**, *43*, 531.

(45) Patterson, J. P.; Robin, M. P.; Chassenieux, C.; Colombani, O.; O'Reilly, R. K. *Chem. Soc. Rev.* **2014**, *43*, 2412.

(46) Jain, S.; Bates, F. S. *Science* **2003**, *300*, 460.

(47) Lu, A.; Moatsou, D.; Longbottom, D. A.; O'Reilly, R. K. *Chem. Sci.* **2013**, *4*, 965.

(48) Lu, A.; Cotanda, P.; Patterson, J. P.; Longbottom, D. A.; O'Reilly, R. K. *Chem. Commun.* **2012**, *48*, 9699.